

Test Verification of LOX/RP-1 High-Pressure Fuel/Oxidizer-Rich Preburner Designs

B.R. Lawver*

Aerojet Liquid Rocket Company, Sacramento, California

High-pressure combustion of fuel-rich and oxidizer-rich LOX/RP-1 propellants was experimentally evaluated using 4.0-in.-diam prototype preburner injectors and chambers. Testing covered the pressure range of 1292 to 2540 psia. Fuel-rich mixture ratios ranged from 0.238 to 0.367; oxidizer-rich mixture ratios ranged from 27 to 48. Performance, gas temperature uniformity, and stability data are presented for two fuel-rich and two oxidizer-rich preburner injectors. One is a conventional like-on-like design, and the other is a platelet design injector. Measured fuel-rich gas composition and C^* performance are in excellent agreement with kinetic model predictions indicating kinetically limited combustion. The oxidizer-rich test results indicate equilibrium combustion as predicted.

Introduction

DURING the past several years increasing priority has been given to the development of an economical space transportation system. Numerous studies have shown that high-pressure liquid oxygen/hydrocarbon (LOX/HC) booster engines offer significant envelope, weight, and payload advantages over current booster systems. These studies¹ identified the need for both fuel-rich and oxidizer-rich preburners to power turbopumps to achieve the required pump discharge pressures approaching 7000 psia.

Previous development experience has highlighted the need for advanced LOX/HC preburner technology. Fuel-rich hydrocarbon preburners have consistently experienced low combustion efficiency and carbon deposition fouling of the gas turbine. Oxidizer-rich preburners have suffered from combustion chamber wall compatibility problems. Metal wall ignition and reaction with the oxidizer-rich environment has caused failures. This test program² was undertaken to address these technical issues to develop a technology base for advanced LOX/HC preburner development.

Two fuel-rich and two oxidizer-rich preburner injectors were tested with LOX/RP-1 to generate performance, stability, and gas temperature uniformity data over a chamber pressure range from 1292 to 2540 psia. The specific objective of the fuel-rich testing was to generate fuel-rich performance and carbon deposition data. The chamber was fitted with instrumentation probes for taking gas samples and measuring gas temperature uniformity. Carbon deposition data were taken by measuring the pressure drop across a turbine simulator flow device. The fuel-rich testing covered a mixture ratio range from 0.238 to 0.367.

The objective of the oxidizer-rich testing was to demonstrate the feasibility of oxidizer-rich preburners and to obtain performance, stability, and gas temperature uniformity data. The oxidizer-rich testing covered a mixture ratio range from 27 to 48.

Experimental Hardware and Test Setup

Test Hardware

The fuel-rich and oxidizer-rich testing was conducted using the same uncooled workhorse hardware. The hardware, shown in Fig. 1, was designed to provide interchangeability of fuel-rich and oxidizer-rich injectors and simulators.

Turbine simulators and main injector manifold pressure drop simulators were provided to evaluate carbon buildup with the fuel-rich gases and material compatibility with the oxidizer-rich gases. Hexagonal turbine blade simulators were used to form a complex flow path. The blade simulator spacings were adjusted by cold flow to provide pressure ratios of 1.3 to 1.5 across the simulators. The oxidizer-rich blade simulators were sprayed with a zirconium oxide coating to improve compatibility.

The fuel-rich main injector simulator is a flat plate with various-size drilled orifices to evaluate pressure drop and the effects of carbon deposition on the inlet of main injector orifices. The oxidizer-rich main injector simulator is a flat plate with a single orifice to simulate pressure drop.

Nickel-lined chamber segments were used at the injector end of the chamber to provide compatibility. The oxidizer-rich liners were coated with zirconium oxide. A radial inlet quarterwave tube acoustic resonator was used to provide transverse-mode high-frequency stability. The 12 resonator cavities were adjusted to depths of 0.65 and 0.45 in., respectively, for the fuel-rich and oxidizer-rich preburners. Turbulence rings were used to damp longitudinal-mode oscillations and to improve gas temperature uniformity. The turbulence rings were placed 5 in. from the injector face. The nickel turbulence rings were coated with zirconium oxide for the oxidizer-rich testing.

Two nozzle throat flanges and two nozzle throat reducers were used to provide the desired chamber pressures. The nozzle throat reducers were used for performance testing prior to insertion of the turbine and main injector simulators. The oxidizer-rich nozzle throat flange and throat reducer were flame sprayed with zirconium oxide coatings.

Two instrumentation rakes were used to measure gas temperature uniformity and gas composition for the fuel-rich testing. Each rake had two gas sample ports and five thermocouple probes.

Platelet coaxial swirler and electrical-discharge machined (EDM) like-on-like (LOL) element injectors were evaluated with both the fuel-rich and oxidizer-rich preburners. The platelet swirler injector concept is shown in Fig. 2. This in-

Presented as Paper 82-1153 at the AIAA/SAE/ASME 18th Joint Propulsion Conference, Cleveland, Ohio, June 21-23, 1982; submitted July 12, 1982; revision received July 15, 1983. Copyright © American Institute of Aeronautics and Astronautics, Inc., 1982. All rights reserved.

*Senior Technical Specialist. PRA-SA-NASA-18 May 1982.

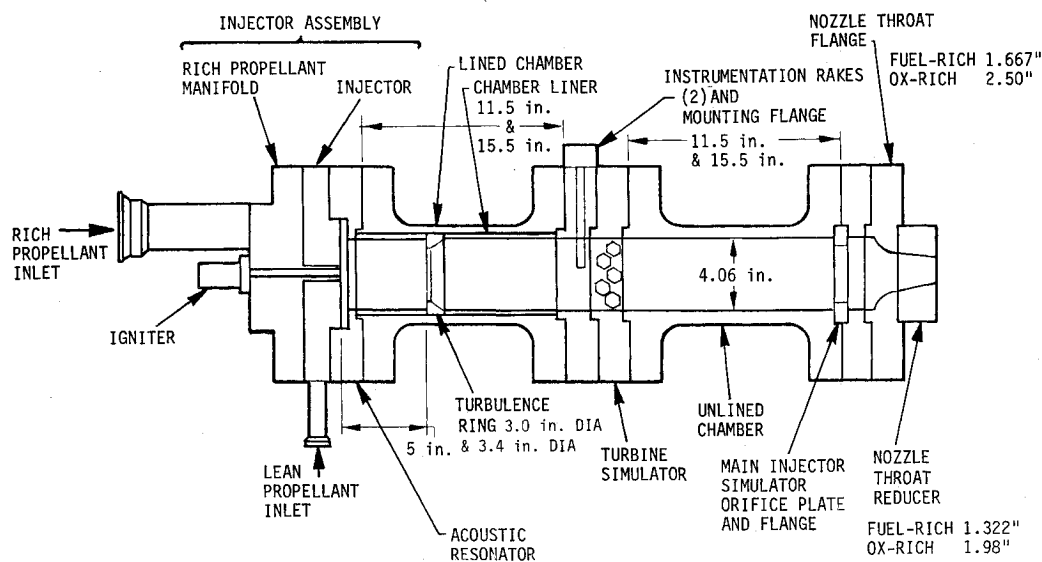


Fig. 1 High-pressure fuel/oxidizer-rich preburner test hardware.

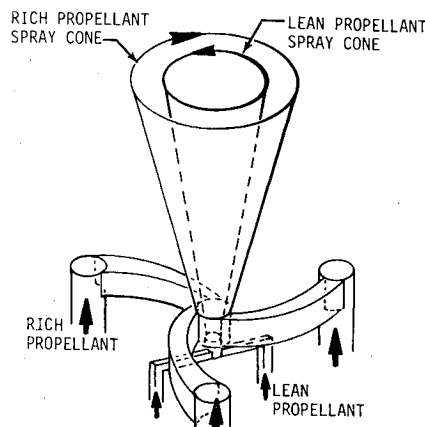


Fig. 2 Platelet swirler injector concept.

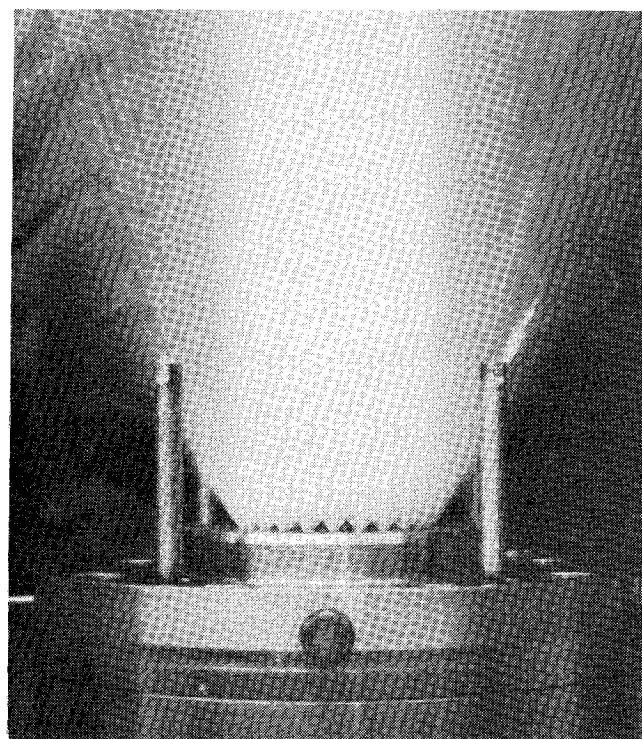


Fig. 3 Water cold flow fuel-rich platelet swirler injector.

jector produces concentric cones of rich and lean propellant. The smaller, lean propellant cone is shrouded by the larger cone of the rich propellant. This injector element was selected on the basis of predicted superior compatibility and gas temperature uniformity, which testing confirmed. However, it exhibits poor ignition characteristics due to shielding of the lean propellant by the rich propellant. Water cold flow of the fuel-rich platelet swirler injector is shown in Fig. 3.

The EDM LOL injector concept is shown in Fig. 4. This injector atomizes the rich propellant with self-impinging LOL elements to form spray fans. The lean propellants are injected through small showerhead elements between the fans. This element was selected to provide a baseline since like-on-like elements are well characterized. Water cold flow of the fuel-rich LOL injector is shown in Fig. 5.

Test Setup

The propellants were fed from high-pressure intensifiers through flow-control valves. The flow-control valves are throttled during the test to permit multiple MR/Pc test points. Both preburners were instrumented to measure C^* performance, stability, and gas temperature uniformity. The fuel-rich preburner was also instrumented to measure preburner gas compositions and turbine simulator carbon deposition.

Ignition was achieved with a GO_2/GH_2 torch igniter.

Combustion Gas Sampling Equipment

Combustion gas compositions for selected fuel-rich tests were measured using the gas probe system shown in Fig. 6.

Combustion gas product specimens were collected in high-pressure sample bombs. The specimens included solid carbon and liquid condensates as well as gas. The gas-phase composition was determined using a gas chromatograph. The solid and liquid fractions were determined by filtration and weighing.

Test Results

Fuel-Rich Preburner

Twenty fuel-rich preburner tests were run over the range of operating conditions listed in Table 1. Sixty-two data points were obtained by running multiple MR/Pc points during the 14-s duration tests. The test results include C^* performance, gas temperature uniformity, stability, gas composition, and material compatibility data. Injector design, chamber pressure, mixture ratio, chamber length, the use of turbulence ring mixing devices, and chamber contraction ratio were evaluated. The chamber pressure was varied over a range

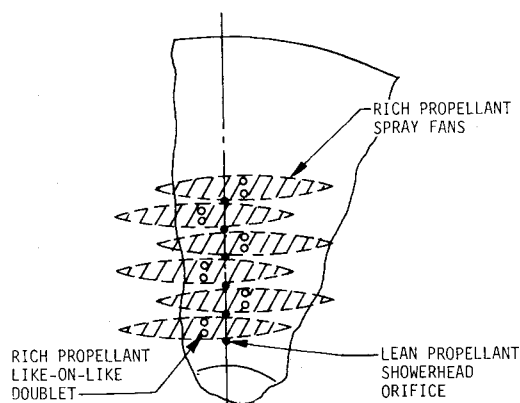


Fig. 4 EDM like-on-like injector concept.

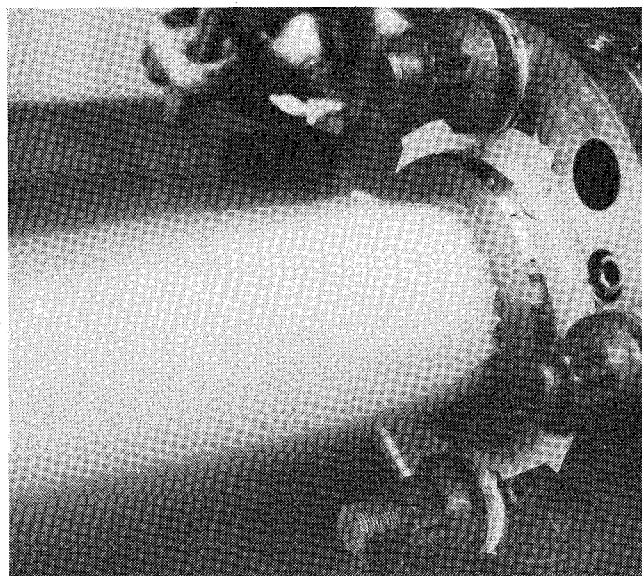


Fig. 5 Water cold flow fuel-rich like-on-like injector.

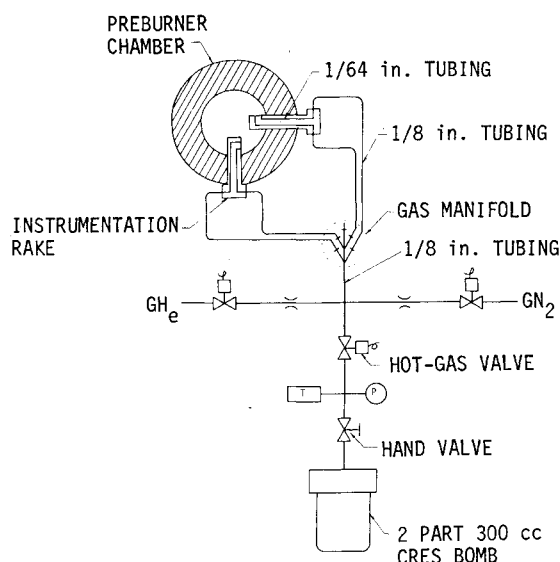
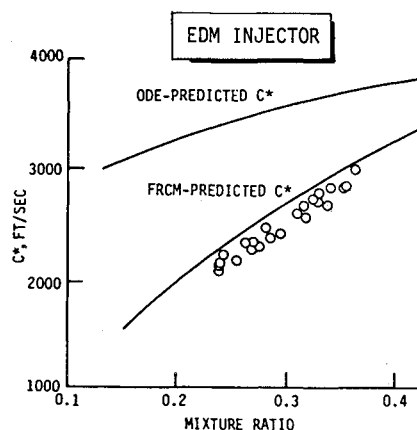


Fig. 6 Fuel-rich combustion gas sampling system.

Fig. 7 Fuel-rich EDM injector measured vs predicted C^* .

from 1292 to 2540 psia. The mixture ratio was varied over a range from 0.238 to 0.367.

The measured C^* and gas composition data were found to be in excellent agreement with a priori predictions made using a previously developed fuel-rich combustion model (FRCM).³ These results indicate that fuel-rich combustion is both kinetically and vaporization limited. Figures 7 and 8 show comparisons of these C^* data with the JANNAF standardized one-dimensional equilibrium (ODE) performance and the FRCM theoretical C^* predictions.

The data show the performance to have little pressure dependence over the range of pressures tested, which is in agreement with the FRCM predictions. The mixture ratio exhibits the single largest effect on C^* level, which is also in agreement with the FRCM predictions. No significant performance differences between injectors is noted.

Energy release efficiencies (ERE) were found to vary from about 62-81% of ODE, depending on mixture ratio. Efficiencies significantly greater than these are not achievable, as evidenced by the close correspondence between the measured C^* and the FRCM-predicted C^* . The measured C^* varies from 92 to 99% of the FRCM-predicted C^* . The C^* is limited by slow fuel decomposition and vaporization.

The effects of the hardware variables on measured C^* are illustrated in Fig. 9 by comparing the EDM injector C^* to the FRCM C^* . Similar effects are observed with the platelet injector. Addition of the turbulence ring mixing device reduces C^* performance. The improved mixing reduces high-

temperature nonuniform gas zones and apparently slows the fuel vaporization.

Reducing contraction ratio increases the C^* performance. The higher chamber gas velocity results in greater gas-to-droplet velocity differentials which speeds vaporization.

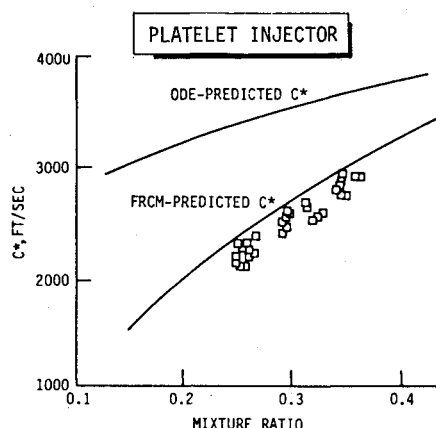
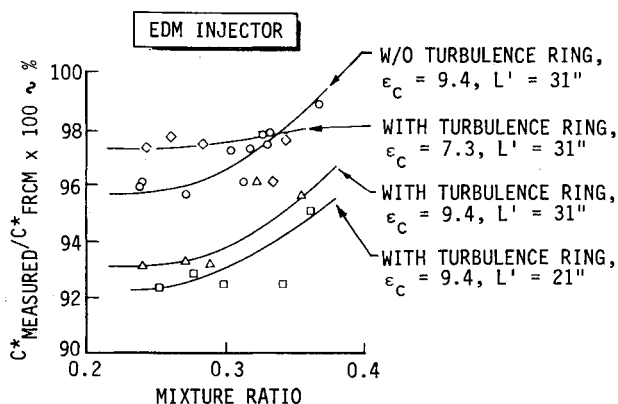
The shape of the C^* performance curves reflects the injector effects on atomization and vaporization. The effect of adding a turbulence ring is the same for the platelet injector as for the EDM injector; performance is reduced for either injector. The platelet injector C^* performance is also enhanced with smaller contraction ratios. Heating the fuel from ambient temperature to approximately 215°F increased the platelet injector C^* performance by about 2%. These observations indicate that vaporization is limiting the kinetic C^* performance at these chamber lengths, which is in agreement with FRCM predictions.

Large amounts of unvaporized fuel are contained in the exhaust, as evidenced by the fuel vaporization efficiencies shown in Fig. 10 and the gas sample test results. Significantly greater vaporization efficiencies do not appear to be achievable due to the kinetically limited gas temperatures which limit vaporization rates.

As shown in Figs. 11 and 12, measured average combustion gas temperatures were found to follow the FRCM predictions. No significant injector effects on average gas temperatures are noted. However, the platelet injector exhibits better gas temperature uniformity than that of the EDM injector when

Table 1 Summary of test points

Fuel-rich Injector	Chamber L' in.	Turbulence ring	Igniter MR	Turbine and main injector simulators	Test duration, s	MR	Pc, psia	No. data tests	No. points
EDM-LOL	31	No	3.5	No	0.5-14	0.25-0.35	1900-2500	5	15
Platelet-swirler	31	No	3.5, 40	No	1-14	0.25-0.35	1900-2500	3	11
Platelet-swirler	21	No	40	No	14	0.25-0.35	1900-2500	2	10
Platelet-swirler	31	Yes (3.0 in.)	40	Yes	14	0.25-0.35	1900-2500	7	11
EDM-LOL	31	No (3.0 in.)	3.5	No	14	0.25-0.35	1900-2500	2	10
EDM-LOL	19	No (3.0 in.)	3.5	No	14	0.25-0.35	1900-2500	1	5
Total					162			20	62
Oxidizer-rich									
EDM-LOL	18	No	40	No	1	37	1900	1	1
Platelet-swirler	18	Yes (3.4 in.)	40	No	0.5	37	No ignition	1	1
Platelet-swirler	18	Yes (3.4 in.)	3.5	No	0.5	37	1840	1	1
Platelet-swirler	18	Yes (3.0 in.)	1.2	No	0.5	36	1870	1	1
EDM-LOL	18	Yes (3.0 in.)	40	No	1	48	2023	1	1
EDM-LOL	18	Yes (3.0 in.)	40	No	0.5	35	Delayed ignition	1	1
EDM-LOL	16	Yes (3.0 in.)	1.2	Yes	0.5-1	33-28	2402-2497	2	2
Total					5			8	8

Fig. 8 Fuel-rich platelet injector measured vs predicted C^* .Fig. 9 Effects of hardware variables on C^* performance.

no turbulence rings are used (see Figs. 13 and 14). With turbulence rings, gas temperature uniformities of better than $\pm 10^\circ\text{F}$ were achieved with both injectors. The influence of the turbulence ring on gas temperature uniformity is dramatic (see Fig. 15) even though the pressure drop across the turbulence ring is only 1-2% (20-50 psid) of chamber pressure. Figure 15 shows data plots of five individual thermocouples with and without the turbulence ring. The radial orientation of the thermocouples (TGP-1, -2, -3, -4, -5) is shown in Fig. 15.

Combustion instabilities in the first and second longitudinal modes were encountered with the platelet injector. These instabilities were effectively damped and controlled by adding turbulence rings and by changing the combustor length. No transverse-mode high-frequency instabilities were incurred since the chambers were provided with tuned acoustic resonators.

Six tests were run with the turbine and main injector simulators installed to evaluate carbon deposition. The preburner was instrumented to measure pressures upstream and downstream of the turbine simulator so that changes in the simulator effective flow areas could be detected. Area reductions during the firing were interpreted to be an indication of carbon buildup. The turbine simulator effective flow areas were calculated by using the measured flow rates and pressures with the isentropic flow relationships. Vaporization efficiency adjustments were made to the measured flow to account for the unvaporized fuel. Multiple points were calculated during each test to determine trends.

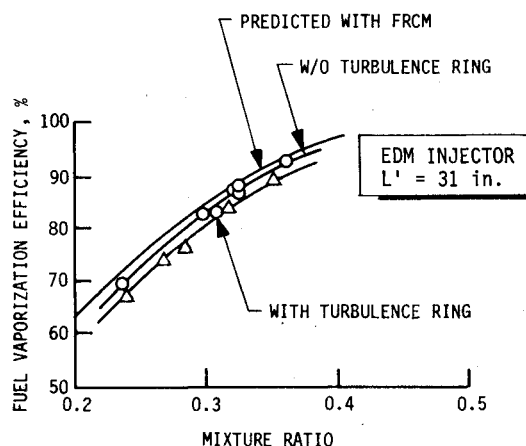


Fig. 10 Fuel-rich EDM injector measured vs predicted fuel vaporization efficiency.

The data indicate flow area reductions during each firing and flow area increases from test to test (see Fig. 16). The area reductions during the test are due to both carbon buildup and thermal expansion of the turbine simulator blades. The flow area increases between tests are due to blade erosion. Therefore it is difficult to accurately define carbon buildup rates. The carbon deposition effects are further clouded by the fact that no significant carbon deposits were found during

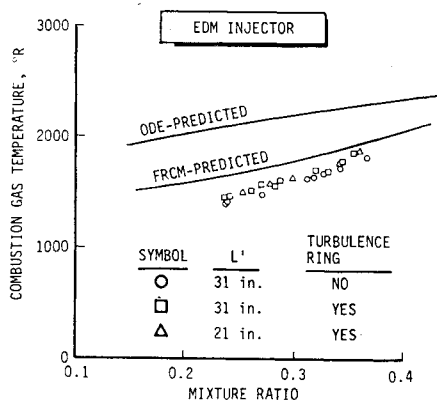


Fig. 11 EDM injector combustion gas temperature—measured average vs predicted.

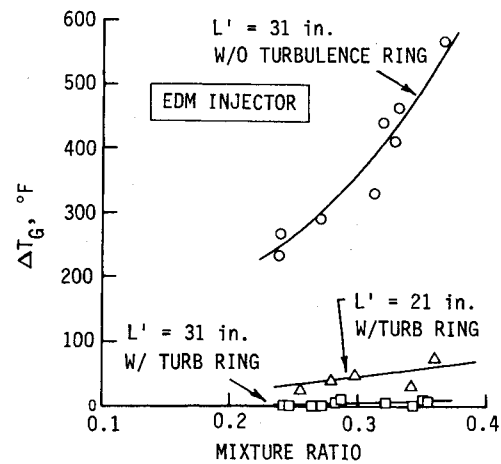


Fig. 13 EDM injector combustion gas temperature uniformity.

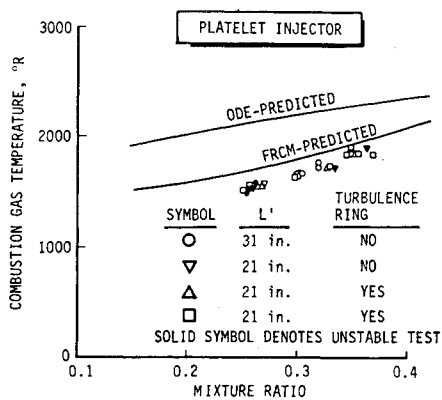


Fig. 12 Platelet injector combustion gas temperature—measured average vs predicted.

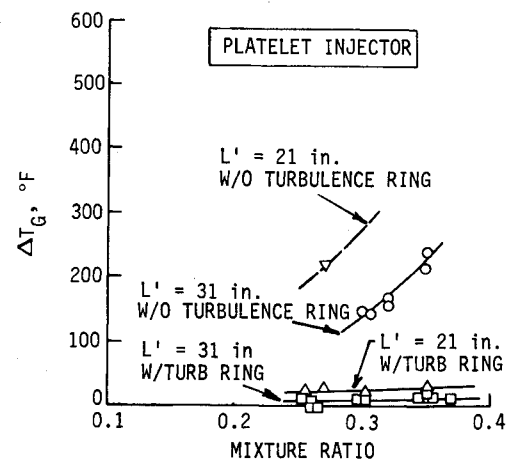


Fig. 14 Platelet injector combustion gas temperature uniformity.

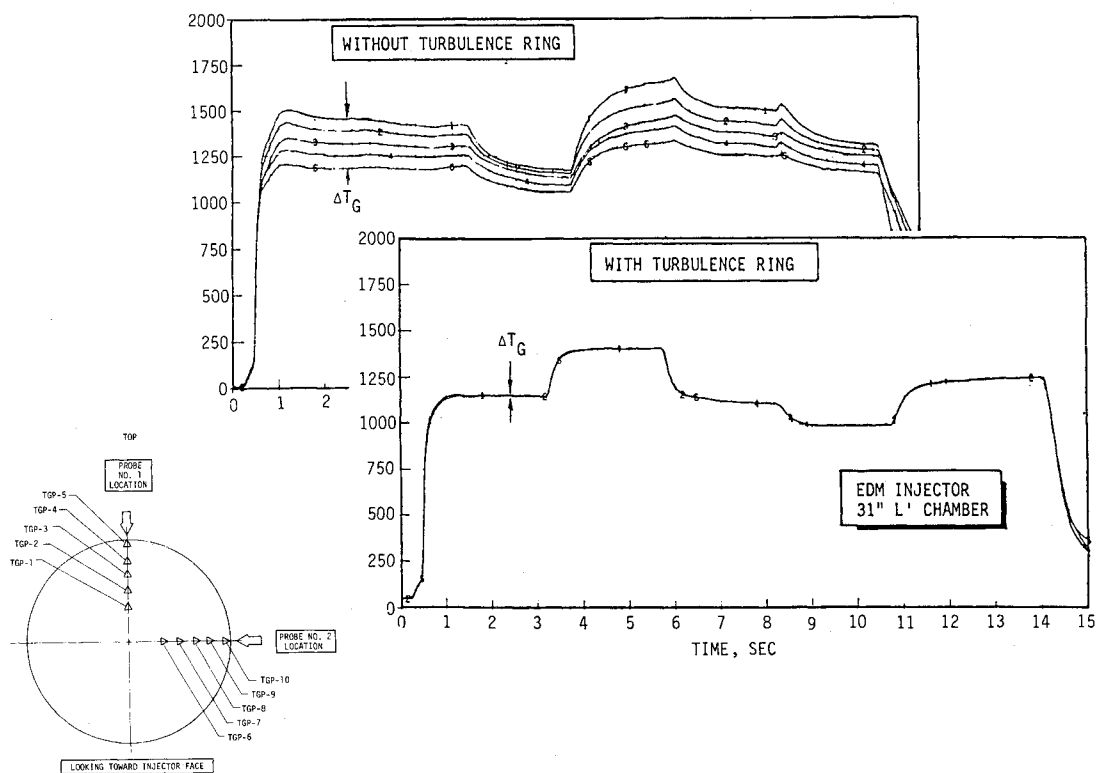


Fig. 15 Effect of turbulence ring on combustion gas temperature uniformity.

post-test examinations and that erosion of the turbine blades had occurred. If the measured area reductions are due to carbon buildup, then the indicated rates are 2-4 times those observed in the early Titan I LOX/RP-1 gas generator. The indicated area reductions vary from 0.13 to 0.25%/s as compared to 0.06%/s for the Titan I gas generator.

Severe erosion of the turbine simulator blades and housing was observed to occur progressively from test to test. The main injector simulator and the nozzle were also badly eroded, with the erosion having the appearance of cavitation damage. Areas of high velocity impingement suffer the worst erosion, as shown in Fig. 17. This effect is also seen in the main injector simulator and nozzle. High-velocity impact seems to aggravate erosion. This form of nozzle throat erosion was observed on all of the fuel-rich testing.

Microhardness tests reveal that the surface layer is softer than the parent material. Softening of the surface indicates

decarburization of the material by the hydrogen-rich (20% by volume) combustion gas. Although decarburization was also observed on the surfaces not subjected to high-velocity flows, there was no evidence of erosion on these surfaces. It is concluded that the high-velocity impact of unvaporized fuel erodes the soft surface allowing progressive softening and erosion.

Oxidizer-Rich Preburner

As listed in Table 1, eight oxidizer-rich tests were completed yielding eight data points. Due to material compatibility problems test durations had to be limited to a maximum of 1 s. Safe start and shutdown were achieved using the valve sequencing shown in Fig. 18. The oxidizer valve is opened to start the sequence. The igniter is timed to start coincident with the filling of the oxidizer manifold, followed by the fuel valve opening. The igniter is terminated during the Pc rise. The shutdown is initiated by closing of the fuel valve. The oxidizer valve lags by 150 ms to ensure an oxidizer-rich shutdown.

The C^* data shown in Fig. 19 confirm that equilibrium combustion is achieved with oxygen-rich preburners as expected. C^* performance of up to 99% of ODE was achieved with the EDM injector.

No gas temperature uniformity data were acquired due to failure of the uncoated thermocouple probes. Serious erosion of uncoated stainless steel materials (nozzle, rake probes, housings) was unexpected, since literature data for static oxygen environments had indicated that temperatures of up to 2300°F can be tolerated by uncoated stainless steel. The maximum gas temperature achieved was about 1900°F, and the maximum wall temperature was estimated to be about 1400°F in a 0.5 s firing. It is concluded that high oxygen gas velocities significantly reduce metal ignition temperatures as compared to static oxygen environments.

Uncoated stainless steel is not compatible with high-velocity oxygen-rich gases at these pressures and temperatures; the nickel and zirconium oxide coated nickel components, on the other hand, exhibited excellent compatibility.

Longitudinal instabilities were incurred but were stabilized with turbulence rings and changes in chamber length. The EDM injector exhibited 1L mode oscillations at 650 Hz in a 16.6 in. L' chamber. Installation of a 3.0-in.-diam turbulence ring and a 13.6-in. chamber length stabilized the EDM injector.

The platelet injector also exhibited 1L mode oscillations in a 17.6-in. L' chamber. Installation of a 3.0-in.-diam turbulence ring stabilized the platelet injector.

FRCM Model Correlations

Gas composition measurements were made and compared to those predicted with the FRCM described in Ref. 3. Except

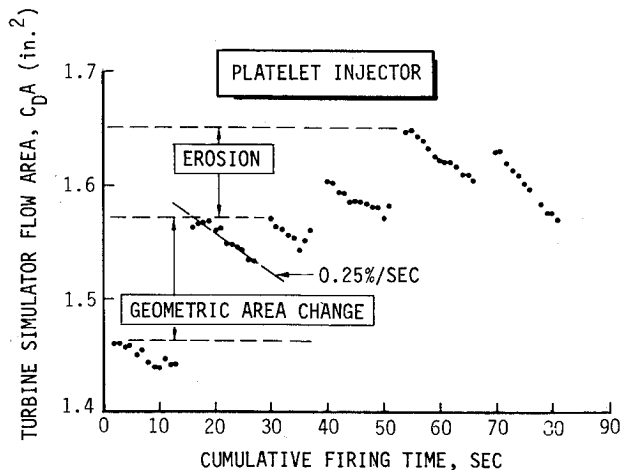


Fig. 16 Turbine simulator flow area history.

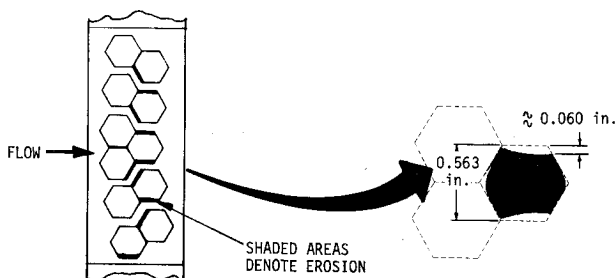


Fig. 17 Turbine simulator blade erosion characteristics.

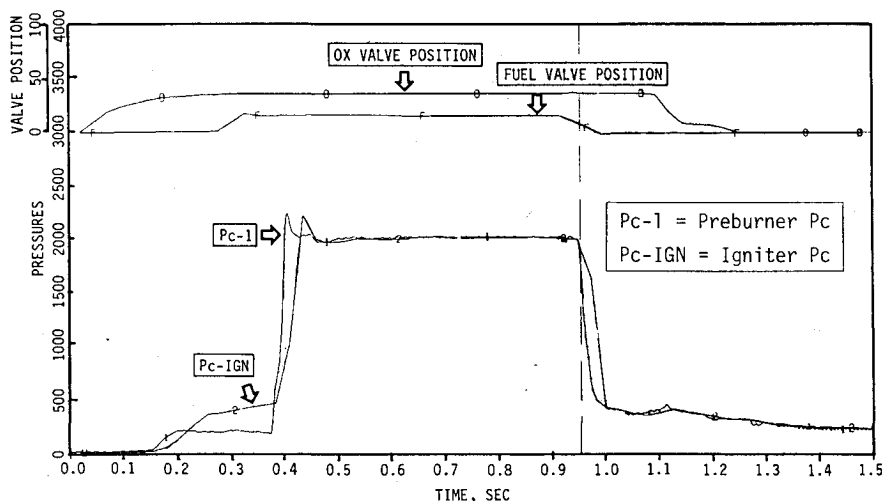
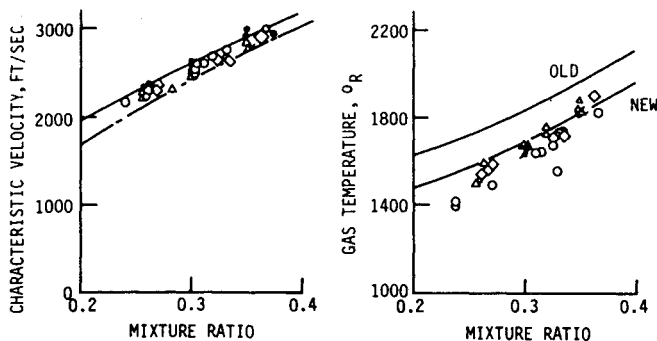
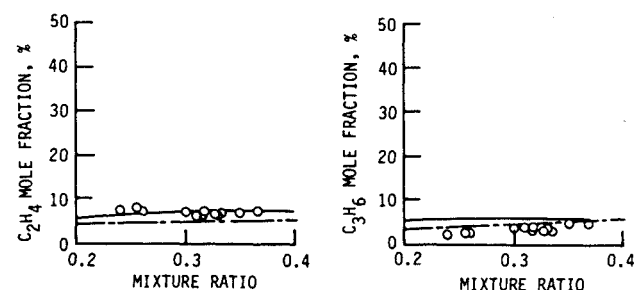
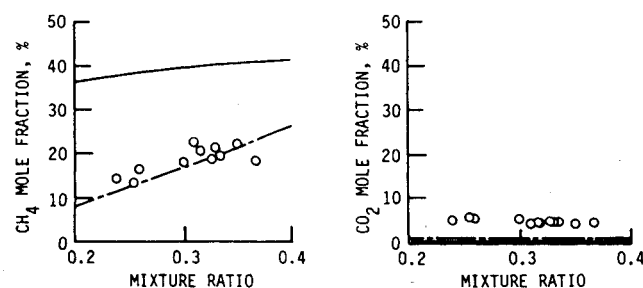
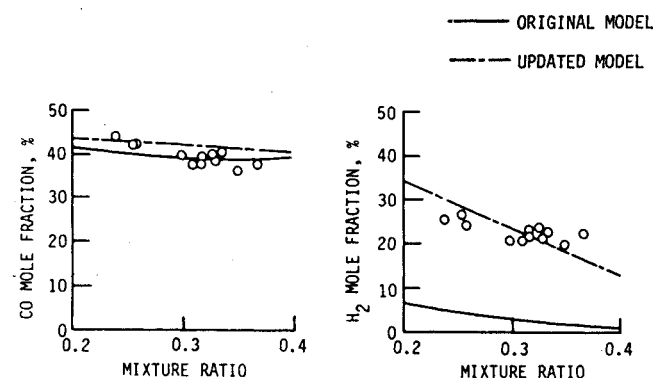
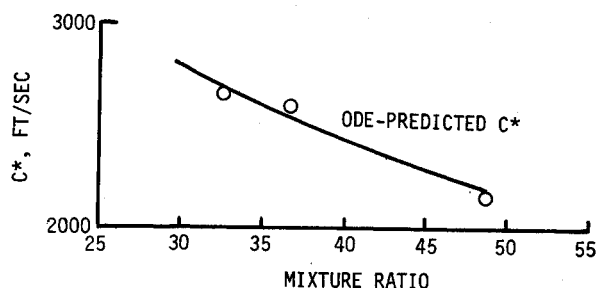


Fig. 18 Oxidizer-rich start and shutdown sequence.



for the CH₄ and H₂ constituents agreement was found to be excellent. A minor modification to one reaction rate constant was required to achieve agreement. Figure 20 shows that the impact on predicted C* performance and gas temperature was small. It is concluded that the FRCM accurately predicts fuel-rich combustion gas properties and performance for engine design purposes.

Conclusions

- 1) Fuel-rich energy release efficiencies (ERE) of 62-81% of ODE were achieved depending on mixture ratio.
- 2) Fuel-rich ERE is limited by slow fuel decomposition kinetics and vaporization.
- 3) Fuel-rich combustion gas properties and C^* performance are predicted accurately with the fuel-rich combustion model.
- 4) Extremely uniform gas temperatures ($\pm 10^\circ\text{F}$) are achievable with low-pressure-loss turbulence rings.
- 5) Longer test durations are required to accurately define fuel-rich carbon deposition effects.
- 6) Fuel-rich turbine and main injector simulator erosion is unacceptably high with the metals used.
- 7) Longitudinal stability with either fuel-rich or oxidizer-rich operation can be achieved with proper turbulence ring and chamber length design.
- 8) Oxidizer-rich preburner operation is difficult to achieve but is believed feasible with proper material selection and operating conditions.

Acknowledgements

This work was supported by Contract NAS 3-22647, Testing of Fuel/Oxidizer-Rich High-Pressure Preburners, NASA/LeRC; Hal Price, Technical Monitor.

References

- ¹O'Brien, C.J. and Ewen, R.L., "Advanced Oxygen-Hydrocarbon Rocket Engine," Final Report, NASA Rept. 33452F, April 1981.
- ²Lawver, B.R., "Testing of Fuel/Oxidizer-Rich High-Pressure Preburners," Final Report, NASA Cr-165609, March 1982.
- ³Schoenman, L., "Fuel/Oxidizer-Rich High-Pressure Preburners," Final Report, NASA CR-165404, Oct. 1981.

U. S. Patent Journal
STATEMENT OF OWNERSHIP, PUBLICATION AND CIRCULATION
Required by 39 U.S.C. 3685

1. TITLE OF PUBLICATION
JOURNAL OF SPACECRAFT AND ROCKETS

2. FREQUENCY OF ISSUE
MONTHLY

3. COMPLETE MAILING ADDRESS OF KNOWN OFFICE OF PUBLISHER (Street, City, County, State and ZIP Code) (For printer)
1513 BROADWAY, NEW YORK, N. Y. 10019

4. COMPLETE MAILING ADDRESS OF THE PUBLISHER (See item 10.37 for not blank)
SAME AS ABOVE

5. COMPLETE MAILING ADDRESS OF PUBLISHER, EDITOR, AND MANAGING EDITOR (See item 10.37 for not blank)
PUBLISHER (Name and Complete Mailing Address):
AMERICAN INSTITUTE OF AERONAUTICS AND ASTRONAUTICS, INC. SAME AS ABOVE
EDITOR (Name and Complete Mailing Address):
R. H. WARECHIE SAME AS ABOVE
MANAGING EDITOR (Name and Complete Mailing Address):

6. FULL NAME _____ COMPLETE MAILING ADDRESS _____
AMERICAN INSTITUTE OF AERONAUTICS **SAME AS ABOVE**
AND ASTRONAUTICS, INC.

7. OTHER (If owned by a corporation, its name and address must be stated and also immediately thereunder the names and addresses of stockholders owning or holding 1 percent or more of total amount of stock. If not owned by a corporation, the names and addresses of the individual owner must be given. If owned by a partnership or other unincorporated firm, its name and address as well as that of each individual must be given. If the publication is published by a proprietor (individual, firm or company), its name and address must be stated (If more than one person is connected with the publication, give the name and address of each person.)

8. KNOWN BONDHOLDERS, MORTGAGEES, AND OTHER SECURITY HOLDERS OWNING OR HOLDING 1 PERCENT OR MORE OF TOTAL AMOUNT OF BONDS, MORTGAGES OR OTHER SECURITIES (If there are none, so state)

9. FOR COMPLETION BY NONPROFIT ORGANIZATIONS SUBMITTING BY MAIL AT SPECIAL RATES (Section 3912 of title 39, U.S.C.)
The purpose, function, and nonprofit status of this organization and the exempt status for Federal income tax purposes (Check one)
☐ HAS NOT CHANGED DURING PRECEDING 12 MONTHS ☐ HAS CHANGED DURING PRECEDING 12 MONTHS (If changed include most complete explanation of change with this statement)

10. EXTENT AND NATURE OF CIRCULATION

	AVERAGE NO. COPIES EACH ISSUE DURING PRECEDING 12 MONTHS	ACTUAL NO. COPIES OF SINGLE ISSUE PUBLISHED NEAREST TO PRECEDING DATE
A. TOTAL NO. COPIES (Net Press Run)	3,683	3,800
B. PAID CIRCULATION		
1. Sales through dealers and carriers, street vendors and counter sales	0	0
2. Mail Subscriptions	3,241	3,504
C. TOTAL PAID CIRCULATION (Sum of B.1 and B.2)	3,241	3,504
D. FREE DISTRIBUTION (Sum of 1, MAIL, CARRIER OR OTHER MEANS SAMPLES, COMPLIMENTARY, AND OTHER FREE COPIES)	63	63
E. TOTAL DISTRIBUTION (Sum of C and D)	3,304	3,567
F. COPIES NOT DISTRIBUTED	379	333
1. Office use, left overs, unclaimed, spoiled after printing		
2. Return from News Agents		
G. TOTAL (Sum of E, F, 1, and 2 - should equal net press run shown in A)	3,683	3,800

11. I certify that the statements made by me above are correct and complete

SIGNATURE AND TITLE OF EDITOR, PUBLISHER, BUSINESS MANAGER, OR OWNER
(Signature)
